Development of the MHD Electrothermal Instability with Boundary Effects

A. H. Nelson*
Imperial College, London, England

An analytic treatment of the linear development of the electrothermal instability with boundary effects is presented. The plasma is assumed to be bounded in one direction only, namely between two parallel walls of finite separation lying parallel to the applied magnetic field. The procedure of the calculation is to Laplace transform the linear electrothermal equations in time, solve the resulting spatial differential equations under the appropriate boundary conditions, and then transform back into real time to obtain the development of a given initial perturbation. Two cases are considered, viz., continuous insulator walls, and infinitely finely segmented electrode walls. In general, an initially plane wave perturbation in the electron density is split into an infinite number of modes, of which usually only a finite number are unstable. As the Hall parameter increases, more and more modes are successively destabilized. However, the critical Hall parameter for destabilization of a given mode usually increases as the wavelength parallel to the walls increases, so that, at least for some geometries, long wavelength perturbations are more stable. In the case of segmented electrodes it may be possible to achieve enhanced stability for a given wavelength by adjusting the external circuitry.

Nomenclature

A,B = matrices in abbreviated form of linearized equations
adj( ) = adjoint of matrix ( )
$\mathbf{B}$ = magnetic field
cf( ) = cofactor of element ( )
d = wall separation
$d\mathbf{s}$ = element of area
$d\mathbf{l}$ = line element
det( ) = determinant of matrix ( )
$\mathbf{E}$ = Lorentz electric field
e = electric charge
h = Planck's constant
I_p = ionization potential of the seed
$\mathcal{I}$( ) = imaginary part of ( )
$\mathbf{j}$ = electrical current density
k = Boltzmann's constant
$\mathbf{K}$ = wave vector
L_o = $12\pi/e^3(\epsilon_o{}^3k^3T_{eo}{}^3/n_{eo})^{1/2}$
l = length of walls in real device
m_i = particle mass of i species
n_i = number density of i species
p_e = electron pressure
R_L = external load resistance
$\mathcal{R}$( ) = real part of ( )
$\mathbf{r}$ = position vector
S = stagger length of diagonally connected segmented electrodes
T_e = electron temperature
T = heavy particle temperature (ions and neutrals)
$\mathbf{u}$ = velocity of heavy particles
w = width of walls in real device
$\hat{\mathbf{x}},\hat{\mathbf{y}}$ = unit vectors in x and y directions
Z = Laplace transform parameter
α = amplitude of initial perturbation
β = Hall parameter
$\Delta\chi$ = range of angles for instability from an infinite plasma theory
$\Delta\theta$ = range of angles spanned by the $\mathbf{K}_E$'s of the instability modes
ϵ_o = permitivity of free space
λ = eigenvalue of Eq. (8)
Λ_i = wavelength in i direction
ν_C = electron-ion collision frequency
ν_B = electron-noble gas collision frequency
ν = $\nu_C + \nu_B$
Π = power output
ϕ = electrostatic potential
ψ = current stream function
σ = plasma electrical conductivity
Θ,Γ = initial amplitudes of instability modes

Subscripts

o = steady-state quantities
e = electrons
s = seed particles
n = noble gas particles
$\perp$ = component perpendicular to the wall
$\parallel$ = component parallel to the wall
x,y = vector components
es = electrostatic
E = effective quantity

Superscripts

$'$ = perturbation quantities
$*$ = fluctuation quantities, $( )^* = ( )'/( )_o$
$-$ = Laplace transform

Received September 5, 1969; revision received February 16, 1970. The author wishes to thank M. G. Haines for some helpful discussions about the work presented here.

* Science Research Council Research Student, Physics Department.

I. Introduction

A PARTIALLY ionized, nonequilibrium plasma in a magnetic field, as envisaged for the working fluid of closed cycle magnetohydrodynamic power generators, is susceptible to the electrothermal or ionization instability. The highly nonuniform distribution of conductivity and Hall parameter that is a consequence of the instability increases the effective internal impedance of the generator, and therefore reduces its performance characteristics.[1,2] It follows that the instability is an important factor in the economics of an MHD generator, and it has therefore been the subject of a considerable amount of both theoretical[3–9] and experimental[10–14] study. A somewhat more complete bibliography of the literature on the electrothermal instability (under the name of Magnetic Striations) has recently been given by Nedasposov.[15]

Most of the theoretical treatments in the past have been linear plane wave analyses of an infinite plasma. This approach has had considerable success in predicting and explaining the experimental observations. In particular the movement of the wave, and the two major stability properties, viz., 1) that the plasma is unstable if the steady-state Hall parameter β_o exceeds a certain critical value and 2) that the wave vector $\mathbf{K}$ for maximum growth satisfies $(\mathbf{j}_o \times \mathbf{K}\cdot\mathbf{B})/(\mathbf{j}_o\cdot\mathbf{K}|\mathbf{B}|) = 1$ for large β_o, are all well understood.

However, experimentally the wavelengths observed have been of the order of the apparatus dimensions, and the growth time is so small that the waves achieve a steady nonlinear level in a time very short compared to the transit time in a generator. In addition, a property of the instability not fully explained by the linear plane wave theories is that the structure of the instability deteriorates from an approximate plane wave to apparently random turbulence as the Hall parameter is increased.[10]

Nonlinear effects and the interaction of the waves with the apparatus walls have therefore had increasing attention in the past two years. For instance, Solbes[2] has given an analytic treatment of the instability including nonlinear terms, while Velikhov et al.[8] and Lengyel[9] have computed numerically the development of the wave to nonlinear levels, applying simple boundary conditions.

The purpose of this paper is to present an analytic treatment of the linear development of the instability under simple boundary conditions. The set of partial differential equations in space and time, obtained by linearizing the pertinent electron and field equations, are solved under boundary conditions on the current density and the electric field. To make the problem mathematically tractable, it is necessary to assume that the plasma is bounded in only one direction perpendicular to the magnetic field. We also make the usual assumption that $\partial/\partial z$ is identically zero for all quantities (where the z direction is parallel to the magnetic field).

The apparatus walls that give rise to the boundary conditions are assumed to lie at $x = 0$ and $x = d$, while the plasma is assumed to be infinite in the y direction. Two cases are examined; 1) insulator walls and 2) infinitely finely segmented electrode walls.

The method of solution employed here is to Laplace transform the equations and boundary conditions in time, and solve the resulting spatial differential equations under the transformed boundary conditions. A similar approach has been used by Dykhne[16] for a bounded plasma of constant conductivity. The Laplace transform method is of course admirably suited to initial value problems, since the initial perturbation enters the calculation via the transform of the time derivative. Applying the inverse Laplace transform to the solution of the transformed equations, we obtain, as a function of space and time, the waves that result from an instantaneous perturbation.

In Sec. II the basic equations of the electrothermal wave phenomenon are described, followed by the presentation of the formal details of the calculation to solve them under any boundary conditions that have the specific topology used here.

The results of the calculations show that in general, an initial plane wave perturbation of electron density is split into an infinite number of electrothermal modes. The amplitudes of the individual modes vary with time in a characteristic way. In general, some grow and some decay, and the structure and properties of the modes for the specific geometries are described in Secs. III and IV.

II. Basic Equations and Analysis

The equations governing the behavior of electrothermal waves are the electron equations (density, energy, and momentum), coupled with the field equations. In the gas frame of a noble gas-alkali metal mixture, these equations are

$$n_e^2/(n_s - n_e) = (2\pi m_e k T_e/h^2)^{3/2} e^{-I_p/kT_e} \tag{1}$$

$$\frac{\partial}{\partial t}\left(\frac{3}{2} n_e k T_e + I_p n_e\right) = \frac{\mathbf{j}^2}{\sigma} - 3n_e k(T_e - T) \times \left(\nu_C \frac{m_e}{m_s} + \nu_B \frac{m_e}{m_n}\right) \tag{2}$$

$$\mathbf{j} = \sigma/(1+\beta^2)(\mathbf{F} + \boldsymbol{\beta}\times\mathbf{F}),\ \mathbf{F} = \mathbf{E} + (1/n_e e)\nabla p_e \quad \text{and} \quad \boldsymbol{\beta} = \mathbf{B}e/m\nu \tag{3}$$

$$\nabla\cdot\mathbf{j} = 0 \tag{4}$$

$$\nabla\times\mathbf{E} = 0 \tag{5}$$

The major assumptions involved in these equations are common to all electrothermal wave analyses, and are discussed at length in Ref. 7.

In addition, we have neglected 1) energy transfer by radiation and thermal conduction, which is a good approximation for the characteristic dimensions used here and 2) the convection and compression terms in the energy equation, which is also a good approximation since these terms contribute only to the movement of the waves, and are usually more than an order of magnitude smaller than the other terms.

The boundary conditions to be satisfied by the vector fields $\mathbf{j}$ and $\mathbf{E}$ are: a) $\mathbf{j}_\perp = 0$ on insulator walls, b) $\mathbf{E}_\parallel = 0$ on electrode walls, and c) if electrode $\epsilon 1$ and electrode $\epsilon 2$ are connected externally by a load R_L, then

$$R_L \int_{\epsilon 1} \mathbf{j}\cdot d\mathbf{s} = -R_L \int_{\epsilon 2} \mathbf{j}\cdot d\mathbf{s} = \int_{\epsilon 2}^{\epsilon 1} \mathbf{E}_{es}\cdot d\mathbf{l}$$

where

$$\mathbf{E}_{es} = \mathbf{E} - \mathbf{u}\times\mathbf{B}$$

We assume that the steady state is uniform in space so that the zero-order equations can be obtained by putting all derivatives to zero in Eqs. (1–5). Equations (4) and (5) are automatically satisfied if we assume $\mathbf{j}$ and $\mathbf{E}$ are of the form $\mathbf{j} = \nabla\times\boldsymbol{\psi}$, $\boldsymbol{\psi} = (0,0,\psi)$, and $\mathbf{E} = -\nabla\phi$.

For electrothermal waves, the assumption is made that the heavy particle properties are constant in space and time (except the degree of ionization).

Linearizing Eqs. (1–5) we can obtain three linear partial differential equations, in x, y, and t, for the variables n_e^*, ψ', and ϕ', assuming that $E_z = 0$ and $\partial/\partial z \equiv 0$ [$\mathbf{B} = (0,0,B) =$ const.]. Assuming that the plasma is infinite in the y direction, we can consider one Fourier component in that direction and replace $\partial/\partial y$ by $-iK_y$. The walls bounding the plasma are assumed to be parallel to the y-z plane, and to lie at $x = 0$ and d. The linearized equations can now be written in the matrix form,

$$\begin{pmatrix} \dfrac{\partial}{\partial t} & -\dfrac{iK_y p_2}{p_1} & 0 \\ \dfrac{q_3 - iK_y q_2}{q_1} & -\dfrac{iK_y q_4}{q_1} & \dfrac{iK_y q_6}{q_1} \\ \dfrac{r_3 - iK_y r_2}{r_1} & 0 & \dfrac{iK_y r_6}{r_1} \end{pmatrix} \begin{pmatrix} n_e^* \\ \psi' \\ \phi' \end{pmatrix} + \begin{pmatrix} 0 & -\dfrac{p_3}{p_1} & 0 \\ 1 & 0 & -\dfrac{q_5}{q_1} \\ 1 & -\dfrac{r_4}{r_1} & -\dfrac{r_5}{r_1} \end{pmatrix} \begin{pmatrix} \dfrac{\partial n_e^*}{\partial x} \\ \dfrac{\partial \psi'}{\partial x} \\ \dfrac{\partial \phi'}{\partial x} \end{pmatrix} = 0$$

where the coefficients (p, q, and r) are functions of the steady-state variables.[17]

In abbreviated notation the equations can be written

$$A(\partial/\partial t)\xi + B(\partial/\partial x)\xi = 0 \tag{6}$$

where ξ is the transpose of (n_e^*, ψ', ϕ') and A and B are the appropriate matrices. The boundary conditions to be satisfied by the linearized quantities are: a) ψ' = constant on insulator walls, b) ϕ' = constant on electrode walls, and c) $R_L\int_{\epsilon 1}\nabla \times \boldsymbol{\psi}'\cdot d\mathbf{s} = -R_L\int_{\epsilon 2}\nabla \times \boldsymbol{\psi}'\cdot d\mathbf{s} = [\phi']_{\epsilon 2}^{\epsilon 1}$. The problem then is to solve Eq. (6) for a given initial perturbation under the boundary conditions appropriate to the system considered.

The Laplace transform of Eq. (6) is

$$A(Z)\bar{\xi} + B\frac{\partial\bar{\xi}}{\partial x} = \eta e^{-i\mathbf{K}\cdot\mathbf{r}} \tag{7}$$

where

$$\bar{\xi}(x,y,Z) = \int_0^\infty \xi(x,y,t)e^{-Zt}dt$$

and η is the transpose of (α,0,0). We have assumed that $n_e^*(x,y,0) = \alpha e^{-i\mathbf{K}\cdot\mathbf{r}}$, i.e., we are applying a plane wave perturbation in the electron density at $t = 0$ and calculating its development in time. (The initial perturbations in ψ' and ϕ' may be obtained by substituting $n_e^*(x,y,0)$ into the two components of the Ohm's Law, and solving for ψ' and ϕ' under the appropriate boundary conditions.) The boundary conditions for $\bar{\psi}'$ and $\bar{\phi}'$ are identical to those for ψ' and ϕ'.

The general solution of Eq. (7) is the sum of the general solution of the reduced equation, i.e.,

$$A(Z)\bar{\xi} + B(\partial\bar{\xi}/\partial\kappa) = 0 \tag{8}$$

together with a particular solution of Eq. (7) itself. The general solution of Eq. (8) is a linear combination of the eigenfunctions $e^{\lambda x}$ where the eigenvalues (λ) are given by

$$\det C(Z,\lambda) = 0, \text{ where } C(Z,\lambda) = A(Z) + \lambda B$$

This equation is a quadratic in λ; hence we can assume then that the general solution of Eq. (8) is of the form

$$\bar{\xi}_i = e^{-iK_y y}\,(\mu_i e^{\lambda_1 x} + \mu_{i+3}e^{\lambda_2 x})$$

where the μ_i's are constant which will be determined by the boundary conditions. A particular solution of Eq. (7) is $\rho e^{-i\mathbf{K}\cdot\mathbf{r}}$ where $D\rho = \eta$, and $D = C(Z, -iK_x)$, i.e., $\rho = D^{-1}\eta = \text{adj}D/\det D\eta$.

The general solution of Eq. (7) is therefore,

$$\bar{\xi}_i = \mu_i e^{\lambda_1 x - iK_y y} + \mu_{i+3}e^{\lambda_2 x - iK_y y} + (D^{-1}\eta)_i e^{-i\mathbf{K}\cdot\mathbf{r}}, \quad i = 1,2,3$$

The μ_i's are determined by the following six linear equations:

$$\begin{pmatrix} 0 & P_{12} & P_{13} & 0 & P_{15} & P_{16} \\ 0 & P_{22} & P_{23} & 0 & P_{25} & P_{26} \\ P_{31} & P_{32} & P_{33} & 0 & 0 & 0 \\ P_{41} & P_{42} & P_{43} & 0 & 0 & 0 \\ 0 & 0 & 0 & P_{54} & P_{55} & P_{56} \\ 0 & 0 & 0 & P_{64} & P_{65} & P_{66} \end{pmatrix}\begin{pmatrix}\mu_1\\ \mu_2\\ \mu_3\\ \mu_4\\ \mu_5\\ \mu_6\end{pmatrix} = \frac{1}{\det D}\begin{pmatrix}\zeta_1\\ \zeta_2\\ 0\\ 0\\ 0\\ 0\end{pmatrix}$$

The first two rows here are simply the formal representation of the boundary conditions, which are linear combinations of $\bar{\psi}'$ and $\bar{\phi}'$, one at $x = 0$, and one at $x = d$. Substituting each of the eigenfunctions into Eq. (8) we obtain two linearly independent homogeneous equations in $\mu_{1,2,3}$ and two in $\mu_{4,5,6}$ these constitute the last four rows. In abbreviated form we have

$$P\mu = \zeta/\det D, \text{ i.e., } \mu = P^{-1}\zeta/\det D$$

Hence the solution for $\bar{\xi}(x,y,Z)$ is

$$\bar{\xi}_i = e^{-iK_y y}\left(\frac{(\text{adj}P\zeta)_i e^{\lambda_1 x} + (\text{adj}P\zeta)_{i+3}e^{\lambda_2 x}}{\det P\det D}\right) + \frac{(\text{adj}D\eta)_i}{\det D}e^{-i\mathbf{K}\cdot\mathbf{r}}$$

To transform back into t space we extend the inverse transform integral

$$\xi(x,y,t) = \frac{1}{2\pi i}\int_{\gamma-i\infty}^{\gamma+i\infty}\bar{\xi}(x,y,Z)e^{Zt}dZ$$

to a path enclosing all space to the left of $\Re(Z) = \gamma$, using the fact that the integrand tends to zero on the semicircle of infinite radius centered at $Z = \gamma$, and lying to the left of $\Re(Z) = \gamma$. Using Laurent's theorem,

$$\xi_i(x,y,t) = \sum_{\text{poles}} (\text{residue of } \bar{\xi}_i \text{ at } Z_{\text{pole}}) \exp(Z_{\text{pole}}t)$$

[γ is such that all singularities, which are simple poles for $\bar{\xi}$, lie to the left of $\Re(Z) = \gamma$.]

The poles of $\bar{\xi}$ are of course given by $\det D(Z) = 0$, and $\det P(Z) = 0$. However, the contribution from the pole at Z_o, the solution of $\det D(Z) = 0$, can be shown to be identically zero for all boundary conditions.[17] $e^{Z_o t}$ is in fact the time dependence of the perturbation $e^{-i\mathbf{K}\cdot\mathbf{r}}$ obtained from an infinite plasma theory. Hence the boundary conditions remove the initial perturbation, and replace it by the modes which are the solution of the dispersion relation,

$$\det P(Z) = 0 \tag{9}$$

and the problem is reduced to solving this equation.

Unstable modes are associated with the solutions with positive real parts, and in the next three sections we will be concerned with the investigation of the spectrum of unstable modes for specific wall types.

III. Insulator Walls

This geometry corresponds to a discharge along the length of a long plasma contained by insulator walls, a situation similar to some instability experiments.[13,15] For insulator walls, boundary condition a reduces to

$$\psi'(x,y) = 0 \text{ at } x = 0,d$$

Because of the periodicity in the y direction, the total perturbed current passing through the plasma is zero, hence $\psi'(0,y) = \psi'(d,y)$; and, since only differences in ψ' are significant, the absolute value of ψ' is arbitrary, and we put $\psi' = 0$ on the walls for convenience. Boundary condition b does not apply since the electrodes lie at $y = \pm\infty$, and c is automatically satisfied by the periodicity in y.

In the steady state $j_{ox} = 0$, and this, together with the boundary conditions, gives a dispersion relation of the form

$$A_{11}(Z)\,[e^{\lambda_1(Z)d} - e^{\lambda_2(Z)d}] = 0$$

Thus we get one pole at $Z = Z_1$, where $A_{11}(Z_1) = 0$, and an infinite number at $Z = Z_{2,3}{}^n$, $n = 1,2,3\ldots$, where $\lambda_1(Z_{2,3}{}^n) - \lambda_2(Z_{2,3}{}^n) = 2\pi in/d$. We have two poles for each n, since the second equation is a quadratic. The value $n = 0$ does not correspond to a pole since the numerator of $\bar{\xi}$ is also zero at the corresponding value of Z; and negative values of n give the same poles as positive values, hence only the latter need be considered. From the residues of $\bar{\xi}$ at these poles we

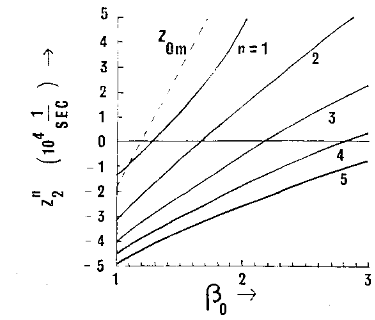

Fig. 1 $\Re$ (Z_2^n) vs Hall parameter (continuous insulator walls).

can write the solution for ξ in the following form:

$$\xi = \left[\Theta_1 e^{\lambda_2(Z_1)x + Z_1 t} + \sum_{n=1}^{\infty}\sum_{m=2}^{3}\sum_{k=1}^{2}\Gamma_{mk}{}^n e^{\lambda_k(Z_m{}^n)x + Z_m{}^n t}\right] \times \alpha e^{-iK_y y} \quad (10)$$

where

$$\Theta_1 = \begin{pmatrix} U_1 \\ V_1 \\ W_1 \end{pmatrix}, \; \Gamma_{m,k}{}^n = \begin{pmatrix} F_{m,k}{}^n \\ G_{m,k}{}^n \\ H_{m,k}{}^n \end{pmatrix}$$

$$U_1 = i\lambda_2(Z_1)/K_x(1 - e^{-iK_x d})/[1 - e^{\lambda_2(Z_1)d}]$$

$$F_{m,k}{}^n = \frac{i\lambda_k(Z_m{}^n)B_{12}\pi ncfD_{12}(-1)^{n+m+k}[(-1)^{n+1} + e^{-[iK_x + \Delta\lambda(Z_m{}^n)d]}](Q_1 Z_m{}^n + Q_2)^2}{\det D(Z_m{}^n)(Z_3{}^n - Z_2{}^n)Q_1\left(Q_1\dfrac{\pi^2 n^2}{d^2} - Q_4\right)A_{11}(Z_m{}^n)d^2}$$

$$V_1 = 0, G_{m,k}{}^n = -\frac{C_{11}[Z_m{}^n, \lambda_k(Z_m{}^n)]}{C_{12}[Z_m{}^n, \lambda_k(Z_m{}^n)]}F_{m,k}{}^n$$

$$W_1 = \frac{\mathrm{cf}C_{13}[Z_1, \lambda_2(Z_1)]}{\mathrm{cf}C_{11}[Z_1, \lambda_2(Z_1)]}U_1, \; H_{m,k}{}^n = \frac{\mathrm{cf}C_{13}[Z_m{}^n, \lambda_k(Z_m{}^n)]}{\mathrm{cf}C_{11}[Z_m{}^n, \lambda_k(Z_m{}^n)]}F_{m,k}{}^n$$

$\Delta\lambda(Z) = \frac{1}{2}[\lambda_1(Z) - \lambda_2(Z)]$ and the Q's are defined by

$$\det C(Z,\lambda) = (Q_1 Z + Q_2)\lambda^2 + Q_3\lambda + (Q_4 Z + Q_5)$$

Equation (10) represents the time development of the initial plane wave perturbation at every point in x and y. At $t = 0$ the sum of the modes is equal to the perturbation, $\alpha e^{-i\mathbf{K}\cdot\mathbf{r}}$; however the amplitude of each mode will vary in time, and in general the form of the initial perturbation will disappear.

The values of Z have been calculated for an Argon-Caesium plasma with the following parameters: $n_n = 10^{25}\ 1/m^3$, $n_s/n_n = 10^{-3}$, $T = 1500°K$, $T_{eo} = 2500°K$, $d = 5$ cm (these parameters have been used in all the calculations reported in this paper).

The real parts of Z_1 and $Z_3{}^n$, $\Re(Z_1)$ and $\Re(Z_3{}^n)$, have been found to be always negative. The Z_1 mode is stable since it has zero ψ' associated with it (see Eq. 10), and hence zero $\mathbf{j}'$. The mode must therefore decay since the source term of the electrothermal instability is the $\mathbf{j}'$ contribution to the perturbed Ohmic heating. Note also that $G_{m1}{}^n = -G_{m2}{}^n$ and therefore ψ' is a sum of $\sin(\pi nx/d)$ terms, i.e., the solution satisfies the boundary conditions.

$\Re(Z_2{}^n)$ is plotted in Fig. 1 as a function of β_o for the least stable modes. (These curves are plotted for $\Lambda_y = 2\pi/K_y = 10$ cm, and the Hall parameter was varied by varying the magnitude of the magnetic field.) We see that as β_o increases the modes are successively destabilized, starting with $n = 1$. For comparison, the broken curve shows $\Re(Z_{om})$. This is the growth rate from the infinite plasma theory for a perturbation $\alpha e^{-i\mathbf{K}_m\cdot\mathbf{r}}$, where $(\mathbf{j}_o \times \mathbf{K}_m\cdot\mathbf{B})/(\mathbf{j}_o\cdot\mathbf{K}_m|\mathbf{B}|) = 1$, i.e., a plane wave oriented in the direction for maximum growth (for large values of β_o). The dispersion relation (9) is in fact independent of K_x, and consequently so are $Z_2{}^n$ and $\lambda_{1,2}(Z_2{}^n)$. However, the initial amplitudes of the modes are obviously K_x dependent.

Each mode is a sum of two plane waves, since the values of $\lambda_{1,2}(Z_2{}^n)$ are purely imaginary, and the form of the instability at $\beta_o = 1.5$ and $\beta_o = 2.2$ are shown in Fig. 2. The second of these pictures is a combination of the modes $n = 1$ and 2, and is a projection of what the nonlinear instability would look like with no mode-mode interaction, and assuming that the nonlinear amplitude of a mode is proportional to its linear growth rate. Mode-mode interaction as well as harmonic generation will of course be important in the nonlinear phase of the instability; however these pictures give some idea of the qualitative features of the instability.

The breakdown of the instability from an approximate plane wave, with one mode present, to apparently random turbulence, as more modes are destabilized, has been well established experimentally,[15] and appears in the results of some of the nonlinear, finite plasma computations.[8] That the turbulent structure is caused by higher periodicities has been previously recognised; in particular, a formula for the modes of ψ' which is equivalent to Eq. (10), without the time dependence, has been given by Shipuk and Pashkin.[10] However, no justification of the successive destabilization of the modes has been given by Shipuk and Pashkin, while the theory presented here shows this phenomenon follows naturally from the application of boundary conditions.

A simple physical picture of why the modes have the behaviour described above can be given on the basis of the plane wave-infinite plasma theory. We know from this theory that, if χ is the angle $\tan^{-1}(\mathbf{j}_o \times \mathbf{K}\cdot\mathbf{B})/(\mathbf{j}_o\cdot\mathbf{K}|\mathbf{B}|)$, then only plane waves with χ in a range of angles $(\Delta\chi)$ around $\pi/4$ or $5\pi/4$ will grow. Now usually the modes are approximately plane waves, and we therefore expect that a similar condition for the stability of a mode will apply if we can define an effective wave vector $\mathbf{K}_E$.

For the $Z_2{}^n$ modes, $\lambda_1 + \lambda_2 \approx 2\pi in/d$ and hence $\lambda_1 \approx 2\pi in/d$ and $\lambda_2 \ll \lambda_1$. $\mathbf{K}_E$ can then be defined as $\mathbf{K}_E = -(2\pi n/d)\hat{\mathbf{x}} + K_y\hat{\mathbf{y}}$, and, since $\mathbf{j}_o$ is parallel to the y axis,

$$\chi_E(n) = \tan^{-1}(2\pi n/dK_y) = \tan^{-1}[n(\Lambda_y/d)]$$

As n increases $\chi_E(n)$ tends to $\pi/2$, therefore the stability of the mode increases with n, since $\mathbf{K}_E$ moves further away from $\mathbf{K}_m$. As β_o increases, $\Delta\chi$ increases,[7] and therefore more and more modes get destabilized as they fall within the range of instability. Note that the fact that $\mathbf{K}_E$ is independent of K_x

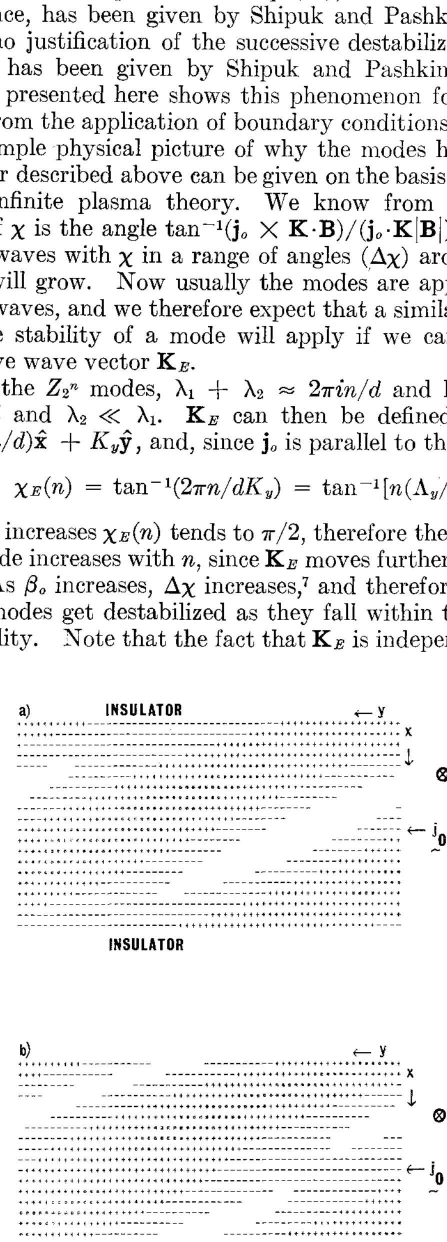

Fig. 2 Contour maps of $n_e{}^*$ in the continuous insulator wall case: a) $\beta_0 = 1.5$, b) $\beta_0 = 2.2$. Asterisk: $n^*_e/n_{e\max}{}^* > 0.9$, plus: $0 < n_e{}^*/n_{e\max}{}^* < 0.9$, minus: $-0.9 < n_e{}^*/n_{e\max}{}^* < 0$, blank: $n_e{}^*/n_{e\max}{}^* < -0.9$ (for both a and b, $\Lambda_y = 10$ cm, $d = 5$ cm).

explains why the stability of the modes is independent of this parameter.

The $Z_3{}^n$ modes are stable since $\lambda_1(Z_3{}^n) + \lambda_2(Z_3{}^n) \approx -2\pi i n/d$ and hence for them $(\mathbf{j}_o \times \mathbf{K}_E\cdot\mathbf{B})/(\mathbf{j}_o\cdot\mathbf{K}_E|\mathbf{B}|) < 0$, i.e., $\mathbf{K}_E$ never falls within $\Delta\chi$.

If Λ_y is increased then, for constant n, $\chi_E(n)$ tends to $\pi/2$ for the $Z_2{}^n$ modes, therefore we expect that perturbations of longer wavelength will be more stable than shorter wavelength perturbations. In Fig. 3 we plot the critical value of the Hall parameter, $\beta_{o\mathrm{crit}}$, against Λ_y/d for various modes. We see that $\beta_{o\mathrm{crit}}$ increases with Λ_y/d, whereas for $\Lambda_y/d \ll 1$, a large number of modes become unstable at, or nearly at, β_∞, which is $\beta_{o\mathrm{crit}}$ for Z_o. As Λ_y tends to zero, $\beta_{o\mathrm{crit}}$ will go through a minimum for low values of n and increase towards infinity. This is because $\chi_E(n)$ tends to zero; but there will always be a high enough value of n such that $\tan\chi_E(n)$ is near enough to 1 for instability. However, the effects of energy transfer, i.e., thermal conduction and radiation, which have been neglected in this analysis, will dominate when Λ_y is less than some characteristic length, typically of the order of 1 mm.[7] And since these effects damp the wave, they will cause $\beta_{o\mathrm{crit}}$ to go to infinite as Λ_y tends to zero for all values of n.

IV. Infinitely Finely Segmented Electrode Walls

This case corresponds to a long Hall or Faraday generator, and we are effectively assuming that the segmentation length is much less than Λ_y. To present as simple results as possible, we will assume that the electrodes are shorted externally, though they may be diagonally connected (see Fig. 4). In this case boundary condition c reduces to

$$\psi'(0,y) = \psi'(d,y + S),\ \phi'(0,y) = \phi'(d,y + S)$$

Since the individual electrode and insulator lengths are assumed to be negligibly small, boundary conditions a and b do not apply.

The dispersion relation is

$$\{\mathrm{cf}C_{12}[\lambda_2(Z)]\mathrm{cf}C_{13}[\lambda_1(Z)] - \mathrm{cf}C_{12}[\lambda_1(Z)]\mathrm{cf}C_{13}[\lambda_2(Z)]\} \times (1 - e^{\lambda_1(Z)d - iK_yS}) = 0$$

The expression in the first set of brackets is a cubic in Z with solutions $Z_{6,7,8}$, and from the other factor of the L.H.S. we get poles at $Z_9{}^n$ which are the solutions of $\lambda_1(Z) = i(2\pi n + K_yS/d)$. The poles give the following solutions for ξ:

$$\xi = \left(\sum_{m=6}^{8}\sum_{k=1}^{2}\Theta_{mk}e^{\lambda_k(Z_m)x + Z_m t} + \sum_{n=-\infty}^{\infty}\Gamma^n e^{\lambda_1(Z_9{}^n)x + Z_9{}^n t}\right)\alpha e^{-iK_y y}$$

where Θ and Γ are defined as before with appropriate indices,

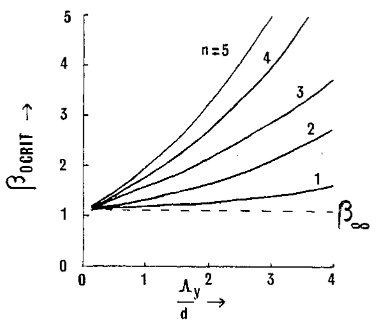

Fig. 3 Critical Hall parameter for various modes vs Λ_y/d (continuous insulator walls). β_∞ is the critical Hall parameter from the infinite plasma theory.

Fig. 4 External circuitry for segmented electrode case.

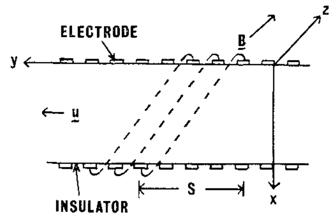

and

$$U_{mk} = \frac{\begin{matrix}(-1)^{k+1}C_{12}[\lambda_k(Z_m)]C_{23}[\lambda_k(Z_m)] \times \\ \{\mathrm{cf}C_{33}[\lambda_l(Z_m)]\mathrm{cf}D_{12} + C_{11}[\lambda_l(Z_m)]\end{matrix}}{\det D(Z_m)[\lambda_1(Z_m) - \lambda_2(Z_m)](Z_m - Z_h)} \times \frac{C_{23}[\lambda_l(Z_m)]\mathrm{cf}D_{13}\}}{(Z_m - Z_j)}$$

$$l = \begin{bmatrix} 2, k = 1 \\ 1, k = 2 \end{bmatrix}$$

and h,j = the combination of 6, 7, 8 not including m.

$$F^n = \frac{\begin{matrix}C_{12}[\lambda_1(Z_9{}^n)]C_{23}[\lambda_1(Z_9{}^n)]\{\mathrm{cf}C_{33}[\lambda_2(Z_9{}^n)]\mathrm{cf}D_{12} + \\ C_{23}[\lambda_2(Z_9{}^n)]C_{11}[\lambda_2(Z_9{}^n)]\mathrm{cf}D_{13}\}\end{matrix}}{\det D(Z_9{}^n)B_{23}A_{22}(Z_9{}^n - Z_6)(Z_9{}^n - Z_7)(Z_9{}^n - Z_8)d} \times \frac{[Q_1(Z_9{}^n) + Q_2]^2\,(1 - e^{liK_yS - iK_xd})}{Q_1\left[\left(\dfrac{2\pi n + K_yS}{d}\right)^2 Q_1 - Q_4\right]}$$

$$V_{mk} = -\frac{C_{11}[Z_m,\lambda_k(Z_m)]}{C_{12}[Z_m,\lambda_k(Z_m)]}U_{mk},\quad G^n = -\frac{C_{11}[Z_9{}^n,\lambda_1(Z_9{}^n)]}{C_{12}[Z_9{}^n,\lambda_1(Z_9{}^n)]}F^n$$

$$W_{mk} = \frac{\mathrm{cf}C_{13}[Z_m,\lambda_k(Z_m)]}{\mathrm{cf}C_{11}[Z_m,\lambda_k(Z_m)]}U_{mk},\quad H^n = \frac{\mathrm{cf}C_{13}[Z_9{}^n,\lambda_1(Z_9{}^n)]}{\mathrm{cf}C_{11}[Z_9{}^n,\lambda_1(Z_9{}^n)]}F^n$$

To calculate the values of Z here we have to establish the ratio j_{oy}/j_{ox} in order to evaluate the elements of A and B. The magnitude of $\mathbf{j}_o$ is fixed by T_{eo}. If the geometry represents a generator of length l ($\gg d$) and width w, and the output current passes through a single load (R_L) connected between the ends of the duct, then,

$$E_{oy} = -[j_{oy} - (S/d)j_{ox}]/\sigma_L, \text{ where } \sigma_L = wd/R_L l$$

On account of the external shorting circuits, we have $E_{ox}d + E_{oy}S = 0$, i.e., $E_{ox} = -S/dE_{oy}$. Substituting these into the steady-state Ohm's Law we obtain,

$$j_{oy}/j_{ox} = [\beta_o + (\sigma_o/\sigma_L)S/d]/(1 + \sigma_o/\sigma_L) \qquad (11)$$

Putting $S = 0$ and maximizing the power output, viz.,

$$\Pi = wld(j_{oy} - j_{ox}S/d)^2/\sigma_L$$

with respect to σ_L, we obtain

$$(\sigma/\sigma_L)_{\max} = 1 + \beta_o{}^2 \text{ and } (j_{oy}/j_{ox})_{\max} = \beta_o/(2 + \beta_o{}^2)$$

Using this value for j_{oy}/j_{ox} we find that $\Re(Z_{6,7,8})$ are all negative, whereas the values of $\Re(Z_n{}^9)$, which are positive, are drawn in Fig. 5 as a function $\beta_o(\Lambda_y = 10$ cm). In Fig. 6 $\beta_{o\mathrm{crit}}$ is drawn as a function of Λ_y/d for the same values of n, while Fig. 7 shows the projected form of the instability at $\beta_o = 3$ and 7.

The $Z_n{}^9$ modes are simple plane waves and the forms of the graphs are compatible with the infinite plasma stability condition on $\mathbf{j}_o$, $\mathbf{K}$ and $\mathbf{B}$. It can be seen that the successive destabilization of modes, and the increase in stability with increasing Λ_y are features of this case also.

The results for the two types of wall presented here have established that the boundary conditions give an infinite set

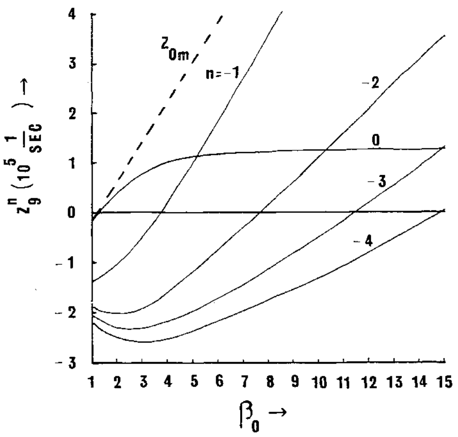

Fig. 5 $\Re\ (Z_{9n})$ **vs Hall parameter (segmented electrode walls).**

of modes, which are either plane waves or nearly plane waves. The effective wave vectors of the modes are all contained within a finite range of angles, $\Delta\theta$ say. We have seen that if $\Delta\theta$ and $\Delta\chi$, the range of angles for instability from an infinite plasma theory, overlap, then the plasma is unstable, with the number of growing modes depending on the amount of overlap.

Can we arrange that $\Delta\theta$ and $\Delta\chi$ do not overlap for arbitrary β_o? In the segmented electrode case we have a circuit parameter, viz., S, with which to attempt this. Here the modes are pure plane waves and the wave vector is given by

$$\mathbf{K}(n) = -\mathscr{I}[\lambda_1(Z_9{}^n)]\hat{\mathbf{x}} + K_y\hat{\mathbf{y}}$$
$$= -[(2\pi n + K_yS)/d]\hat{\mathbf{x}} + K_y\hat{\mathbf{y}},\ n = -\infty, \ldots, \infty$$

if $K_yS/2\pi = N \pm \delta$, where N is the nearest integer to $K_yS/2\pi$, then, defining θ to be the angle $\mathbf{K}(n)$ makes with the x axis, $\Delta\theta$ is the range from $\tan^{-1}(\pm dK_y/2\pi\delta)$ through $\theta = 0$ to $\tan^{-1}[\pm dK_y/2\pi(\delta - 1)]$.

Thus $\Delta\theta$ is grouped around the x axis, and to keep $\Delta\chi$ and $\Delta\theta$ as far apart as possible, for large values of β_o, we require $\mathbf{K}_m$ to lie along the y axis. This requires $j_{oy}/j_{ox} = 1$, i.e., $\sigma/\sigma_L = (\beta_o - 1)/(1 - S/d)$; in order to keep σ_L positive we consider only negative values of S here. For $\mathbf{K}_m$ along the y axis, $\Delta\chi$ and $\Delta\theta$ have least overlap, at large values of β_o, when δ takes its maximum value, i.e., $\delta = \frac{1}{2}$. Then, for $N = 0$ and negative S, we have $S/\Lambda_y = -\frac{1}{2}$.

Setting $j_{oy}/j_{ox} = 1$ we have plotted in Fig. 8 the value of β_{ocrit} for the first mode to destabilize at each point as a function of S/Λ_y, using various values of Λ_y/d. Since the maximum value of $\Delta\chi$ is $\pi/2$, $\Delta\chi$ and $\Delta\theta$ never overlap when $\Lambda_y/d = 2$ and $\delta = S/\Lambda_y = -\frac{1}{2}$, for in this case $\Delta\theta$ is symmetrical about x and equal to $\pi/2$. Hence β_{ocrit} goes to infinity.

Experimentally Λ_y/d is usually observed to lie between 1 and 2, and for $\Lambda_y/d < 2$ β_{ocrit} is always finite, although a pronounced peak in β_{ocrit} is still present. The position of this peak moves further away from $S/\Lambda_y = -\frac{1}{2}$ as the peak value of β_{ocrit} decreases. This is because χ_m is really given by

$$\chi_m = \pi/4 + [1 - \nu_{co}/\nu_o(1 - 1/2\ \log L_o)]/2\beta_o$$
$$\text{or } 5\pi/4 + [1 - \nu_{co}/\nu_o(1 - 1/2\ \log L_o)]/2\beta_o$$

and hence, for low values of β_o, the direction for maximum growth is not quite along the y axis when $j_{oy}/j_{ox} = 1$. Consequently there is minimum overlap between $\Delta\theta$ and $\Delta\chi$ when $\Delta\theta$ is not quite symmetrical about $\theta = 0$, i.e., S/Λ_y is not quite $-\frac{1}{2}$, since minimum overlap occurs when $\Delta\theta$ is symmetrical about a line perpendicular to the direction for maximum growth.

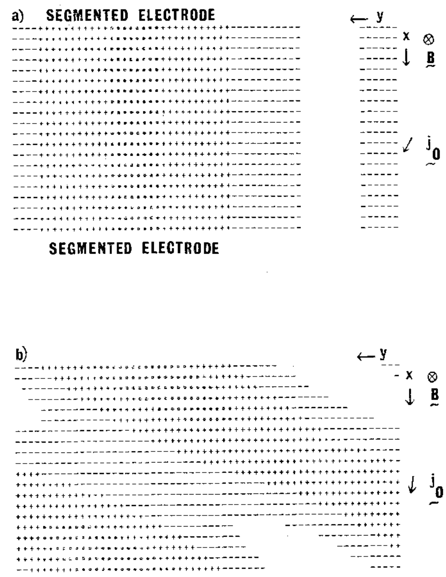

Fig. 7 Contour maps of n_e* in the segmented electrode case: a) $\beta_0 = 3$, b) $\beta_0 = 7$. Asterisk: $ne^*/n_{emax}^* > 0.9$, plus: $0 < n_e^*/n_{emax}^* < 0.9$, minus: $0 < n_e^*/n_{emax}^* < -0.9$, blank: $n_e^*/n_{emax}^* < -0.9$. (for both a and b), $\Lambda_y = 10$ cm, $d = 5$ cm).

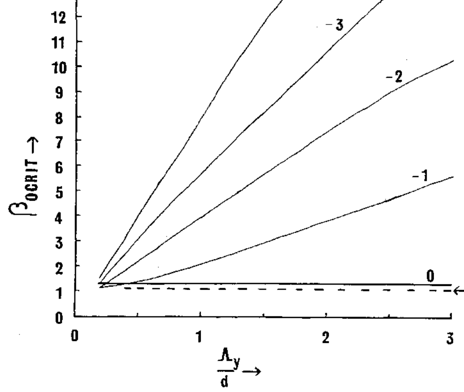

Fig. 6 Critical Hall parameter for various modes vs $\Lambda y/d$ (segmented electrode walls).

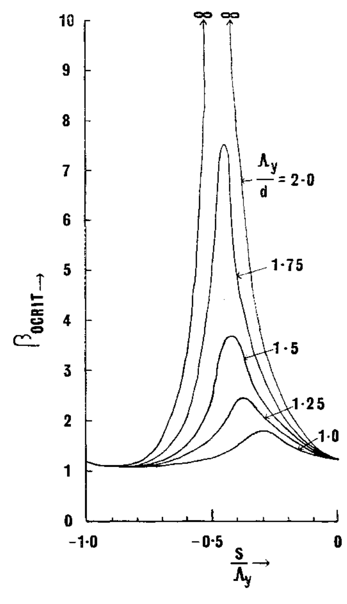

Fig. 8 Smallest critical Hall parameter vs. S/Λ_y for various values of Λ_y/d.

We see therefore that, by a suitable choice of the parameters R_L and S, a significant stabilizing effect can be achieved for the case of shorted segmented electrodes. S must be taken near to $-\Lambda_y/2$, and R_L must then be chosen such that $\mathbf{K}_m$ is near to the y axis. This means, however, that the value of σ_o/σ_L is not equal to $(\sigma_o/\sigma_L)_{\max}$. If the object of stabilizing the waves is to increase the output power of the generator, a compromise between stabilization and load optimization may be necessary. It also must be noted that this technique will apply to only one value of Λ_y; however, in practice often one dominant value of Λ_y seems to appear.[10,14]

V. Summary

The linear analysis of the electrothermal instability presented in this paper shows that the boundary walls of a finite plasma can have a considerable effect on the instability. In general, a plane wave perturbation in the electron density is split into an infinite number of modes. These modes are plane waves in the case of externally shorted, finely segmented electrodes, and approximate plane waves in the cases of continuous insulator walls. Usually only a finite number of the modes are unstable, and this number increases with increasing Hall parameter. The modes have different orientations with respect to the walls, and the successive mode destabilization with increasing Hall parameter provides a plausible explanation for the experimentally observed transition from near plane wave to turbulent structure. Usually the effect of the boundaries is to stabilize perturbations of long wavelength, so that if the effects of energy transfer are taken into account, the critical Hall parameter has a minimum as a function of wavelength. This is not the case, however, for the segmented electrode geometry with $S = 0$ and external shortings, where $\beta_{o\mathrm{crit}}$ for $n = 0$ does not increase with increasing Λ_y.

The stability of the individual modes can usually be explained in terms of an effective wave vector $\mathbf{K}_E$, which is the wave vector of the plane wave to which the mode approximates. For the mode to be unstable, $\mathbf{K}_E$ must lie within the range of angles for instability $\Delta\chi$ derived from the infinite plasma theory.

In general, the $\mathbf{K}_E$'s of all the modes occupy a range of angles $\Delta\theta$, and the possibility arises of arranging the boundary conditions and external circuitry such that $\Delta\theta$ and $\Delta\chi$ do not overlap till as high a value of Hall parameter as possible. By varying the diagonal connections and the external load of the segmented electrode system considered in Sec. IV, it was shown that enhanced stability could be achieved in this case.

Whether or not this could be achieved in a real system depends on whether or not the boundary conditions dominate over the effects neglected in this analysis. In particular, if the steady state is nonuniform (for example there may exist a layer of hot electrons along the walls) then new or modified constraints may be imposed on the instability. However, the stabilization effect is quite marked for wavelengths equal to or greater than 1.25 times the wall separation, and it seems likely that some stability enhancement may be possible if the plasma steady state is not extremely nonuniform.

References

[1] Rosa, R. J., "Hall and Ion-Slip Effects in a Nonuniform Gas," *The Physics of Fluids*, Vol. 5, No. 9, Sept. 1962, pp. 1081–1090.

[2] Solbes, A., "Quasi-Linear Plane Wave Study of Electrothermal Instabilities," *Proceedings of Symposium on Magnetohydrodynamic Electrical Power Generation*, I.A.E.A., Warsaw, Vol. 1, 1968, pp. 499–518.

[3] Velikhov, E. P. and Dykhne, A. M., "Plasma Turbulence due to the Ionization Instability in a Strong Magnetic Field," *VI Conference Internationale sur les Phenomenes d'Ionisation dans les Gaz*, Paris, Vol. 4, 1963, pp. 511–512.

[4] Kerrebrock, J. L., "Nonequilibrium Ionization due to Electron Heating," *AIAA Journal*, Vol. 2, No. 6, June 1964, pp. 1072–1087.

[5] Nedaspasov, A., "Velocity of Ionization Waves in a Low-Temperature Plasma," *Electricity from MHD, Proceedings of a Symposium*, I.A.E.A., Salzburg, Vol. 2, 1966, pp. 345–348.

[6] Hougen, M. L., "Magnetohydrodynamic Waves in a Weakly Ionized, Radiating Plasma," Ph.D. thesis, June 1968, Dept. of Aeronautics & Astronautics, Massachusetts Institute of Technology, Cambridge, Mass.

[7] Nelson, A. H. and Haines, M. G., "Analysis of the Nature and Growth of Electrothermal Waves," *Plasma Physics* (*Journal of Nuclear Energy*, Part C), Vol. 11, Oct. 1969, pp. 811–837.

[8] Velikhov, E. P. et al., "Numerical Experiment on Ionization Instability Development in a Low Temperature Magnetized Plasma," *Proceedings of 10th Symposium on Engineering Aspects of Magnetohydrodynamics*, Cambridge, Mass., March 1969, pp. 1–4.

[9] Lengyel, L. L., "On the Numerical Simulation of Ionization Instability," *10th Symposium on Engineering Aspects of Magnetohydrodynamics*, Cambridge, Mass., March 1969, supplementary paper.

[10] Shipuk, I. Y. and Pashkin, S. V., "Characteristics of an Unstable Quasi-Equilibrium in Crossed Electric and Magnetic Fields," *Electricity from MHD, Proceedings of a Symposium*, I.A.E.A., Warsaw, Vol. 1, 1968, pp. 569–580.

[11] Zukoski, E. E. and Gilpin, R. R., "Large Amplitude Electrothermal Waves in a Non-equilibrium Plasma," *The Physics of Fluids*, Vol. 10, No. 9, Sept. 1967, pp. 1974–1980.

[12] Louis, J. F., "High Hall Coefficient Experiments in a Large Disk Generator," *Electricity from MHD, Proceedings of a Symposium*, I.A.E.A., Warsaw, Vol. II, 1968, pp. 825–849.

[13] Kerrebrock, J. L. and Dethlefson, R., "Experimental Investigation of Fluctuations in a Nonequilibrium Plasma," *AIAA Journal*, Vol. 6, No. 11, Nov. 1968, pp. 2115–2121.

[14] Brederlow, G. and Hodgson, R. T., "Electrical Conductivity in Seeded Noble Gas Plasmas in Crossed Electric and Magnetic Fields," *AIAA Journal*, Vol. 6, No. 7, July 1968, pp. 1277–1284.

[15] Nedaspasov, A. V., "Striations," *Soviet Physics*, Uspekhi, Vol. 11, No. 2, Sept.–Oct. 1968, pp. 174–187.

[16] Dykhne, A. M., "Ionization Instability in a Bounded Region," *Electricity from MHD, Proceedings of a Symposium*, I.A.E.A., Warsaw, Vol. 1, 1968, pp. 569–580.

[17] Nelson, A. H., "Wave Propagation and Instabilities in a Magnetized, Partially Ionized Gas under Non-Equilibrium Conditions," Ph.D. thesis, 1969, Dept. of Physics, Imperial College of Science & Technology, London, England.